Original Article

Association of artificial intelligence-based high-resolution computed tomography parameters with all-cause mortality in patients with connective tissue disease-associated interstitial lung disease: a longitudinal cohort study

Chen Chu[1], An Yan[2], Jingyu Xu[1], Jun Hu[1], Ying Wei[3], Feng Shi[3], Shengnan Zhao[4], Xiaoyan Xin[1,2]

[1]Department of Radiology, Nanjing Drum Tower Hospital, Affiliated Hospital of Medical School, Nanjing University, Nanjing, China; [2]Department of Radiology, Nanjing Drum Tower Hospital Clinical College of Nanjing Medical University, Nanjing, China; [3]Department of Research and Development, Shanghai United Imaging Intelligence Co., Ltd., Shanghai, China; [4]Department of Rheumatology, Nanjing Drum Tower Hospital, Affiliated Hospital of Medical School, Nanjing University, Nanjing, China

Contributions: (I) Conception and design: C Chu, X Xin; (II) Administrative support: A Yan, J Xu, J Hu, Y Wei, F Shi, S Zhao; (III) Provision of study materials or patients: A Yan, J Xu, S Zhao; (IV) Collection and assembly of data: C Chu, A Yan, J Xu; (V) Data analysis and interpretation: C Chu, A Yan, Y Wei, F Shi; (VI) Manuscript writing: All authors; (VII) Final approval of manuscript: All authors.

Correspondence to: Xiaoyan Xin, PhD. Department of Radiology, Nanjing Drum Tower Hospital, Affiliated Hospital of Medical School, Nanjing University, No. 321 Zhongshan Road, Nanjing 210008, China; Department of Radiology, Nanjing Drum Tower Hospital Clinical College of Nanjing Medical University, Nanjing, China. Email: xinxy98@163.com.

Background: The severity of interstitial lung disease (ILD) is frequently linked to poorer outcomes and reduced quality of life in connective tissue disease-associated ILD (CTD-ILD) patients. The purpose of this study is to investigate the utility of artificial intelligence (AI)-based quantitative high-resolution computed tomography (HRCT) analysis in assessing the prognosis of patients with CTD-ILD.

Methods: This retrospective study included 116 CTD-ILD patients who underwent HRCT scans. Patients were stratified into mild, moderate, and severe groups based on pulmonary function test (PFT) results. Differences in the 17 AI parameters across the three groups were evaluated using one-way analysis of variance (ANOVA) followed by least significant difference (LSD) post hoc pairwise comparisons. The Spearman rank correlation test was employed to examine the association between the 17 AI parameters and pulmonary function grades. Overall survival rates were compared using Kaplan-Meier analysis and ANOVA. Univariate analysis and Cox proportional-hazards regression were used to assess the association between AI-derived parameters and prognosis.

Results: The 17 AI parameters exhibited significant variations across the three groups. Among them, three pulmonary volume parameters were negatively correlated with lung function, while fourteen pulmonary parenchymal involvement parameters were positively correlated with pulmonary function. Significant differences in overall survival rates were observed among the mild, moderate, and severe groups. Univariate analysis revealed that there were 12 indicators showing significant differences between the survival group and the death group. The Cox proportional-hazards regression revealed that the two most important factors were left lung volume and the percentage of disease components ≤–751 Hounsfield units (HU), which were protective factors and risk factors for overall survival rate, respectively.

Conclusions: The quantitative HRCT analysis based on AI can be used to evaluate patients with CTD-ILD and is correlated with overall survival rate.

Keywords: Interstitial lung disease (ILD); connective tissue disease (CTD); artificial intelligence (AI); high-resolution computed tomography (HRCT)

Submitted Sep 04, 2025. Accepted for publication Nov 25, 2025. Published online Jan 20, 2026.
doi: 10.21037/jtd-2025-1827
View this article at: https://dx.doi.org/10.21037/jtd-2025-1827

Introduction

The lungs are a commonly affected organ in connective tissue diseases (CTDs), with CTD-associated interstitial lung disease (CTD-ILD) being a primary manifestation. Among the various pulmonary complications of CTD, interstitial lung disease (ILD) is one of the most prevalent and is associated with significant morbidity and mortality (1,2). Therefore, all CTD patients should undergo ILD evaluation at initial presentation and at regular intervals thereafter. The management of CTD-ILD often differs substantially from that of other primary ILD, such as idiopathic pulmonary fibrosis (IPF) (3). Additionally, the severity of ILD is frequently linked to poorer outcomes and reduced quality of life in CTD-ILD patients (1).

Pulmonary function test (PFT) and high-resolution computed tomography (HRCT) of the chest are the primary methods for clinically assessing disease progression in patients with CTD-ILD (4). PFTs are widely used for screening and monitoring disease activity and progression. Although reduced diffusing capacity of the lungs for carbon monoxide is nonspecific, it is often the earliest physiological indicator of ILD. However, PFT results correlate weakly with the extent of ILD and may be influenced by comorbid conditions. Additionally, some patients with severe ILD are unable to perform PFT adequately due to physical limitations (5,6). HRCT is highly sensitive in detecting CTD-ILD manifestations, such as interlobular septal thickening and ground-glass opacities, which play a crucial role in prognostic evaluation (7). Nevertheless, conventional computed tomography (CT) assessment is susceptible to variability based on the radiologist's subjective interpretation and diagnostic expertise. Consequently, there is a pressing need for an effective quantitative method to improve prognostic evaluation.

In recent years, artificial intelligence (AI) analysis has emerged as a prominent research focus (8), demonstrating its capability to analyze data accurately and quickly, thereby significantly enhancing the efficiency and accuracy of image interpretation (9,10). However, quantitative AI analysis has not yet been applied to prognostic assessments in patients with CTD-ILD. This study utilizes the United Imaging AI system to evaluate total lung volume, as well as the volumes and percentages of lesions in both lungs and individual left/right lungs. Additionally, it examines the composition and proportional distribution of these lesions. We attempted to identify the risk factors and protective factors for the mortality rate of CTD-ILD patients through univariate analysis and Cox proportional-hazards regression. We present this article in accordance with the STROBE reporting checklist (available at https://jtd.amegroups.com/article/view/10.21037/jtd-2025-1827/rc).

Highlight box

Key findings

- This study found that artificial intelligence (AI)-based quantitative high-resolution computed tomography (HRCT) analysis effectively predicts survival in connective tissue disease-associated interstitial lung disease (CTD-ILD) patients. Key independent prognostic factors were left lung volume (a protective factor) and the percentage of diseased lung with attenuation ≤−751 Hounsfield units (a risk factor). Patients with poorer lung function had significantly lower survival rates, and most AI parameters correlated strongly with functional severity.

What is known and what is new?

- HRCT and pulmonary function tests are standard for CTD-ILD assessment but have limitations in subjectivity and prognostic precision.
- This study newly establishes the prognostic value of specific, automated AI-derived HRCT metrics—most notably left lung volume and low-attenuation lesion burden—for predicting long-term mortality in CTD-ILD, moving beyond qualitative pattern description.

What is the implication, and what should change now?

- AI quantification provides an objective tool for risk stratification. Clinicians should consider integrating these specific AI parameters into the multidisciplinary management of CTD-ILD to improve prognostic accuracy and personalize patient monitoring. Future work must validate these biomarkers in larger, prospective, multi-center studies to enable their clinical adoption and model development.

Methods

Subjects

This retrospective study enrolled patients with CTD-ILD admitted to the Rheumatology and Immunology Department of Nanjing Drum Tower Hospital between January 2017 and December 2018. This study was conducted in accordance with the Declaration of Helsinki and its subsequent amendments. The study was approved by the Ethics Committee of Nanjing Drum Tower Hospital (No. 2022-449-02) and informed consent was obtained from the participants' next of kin or directly from the patients. A comprehensive review of their HRCT data was performed, followed by a 6-year follow-up. Inclusion criteria: (I)

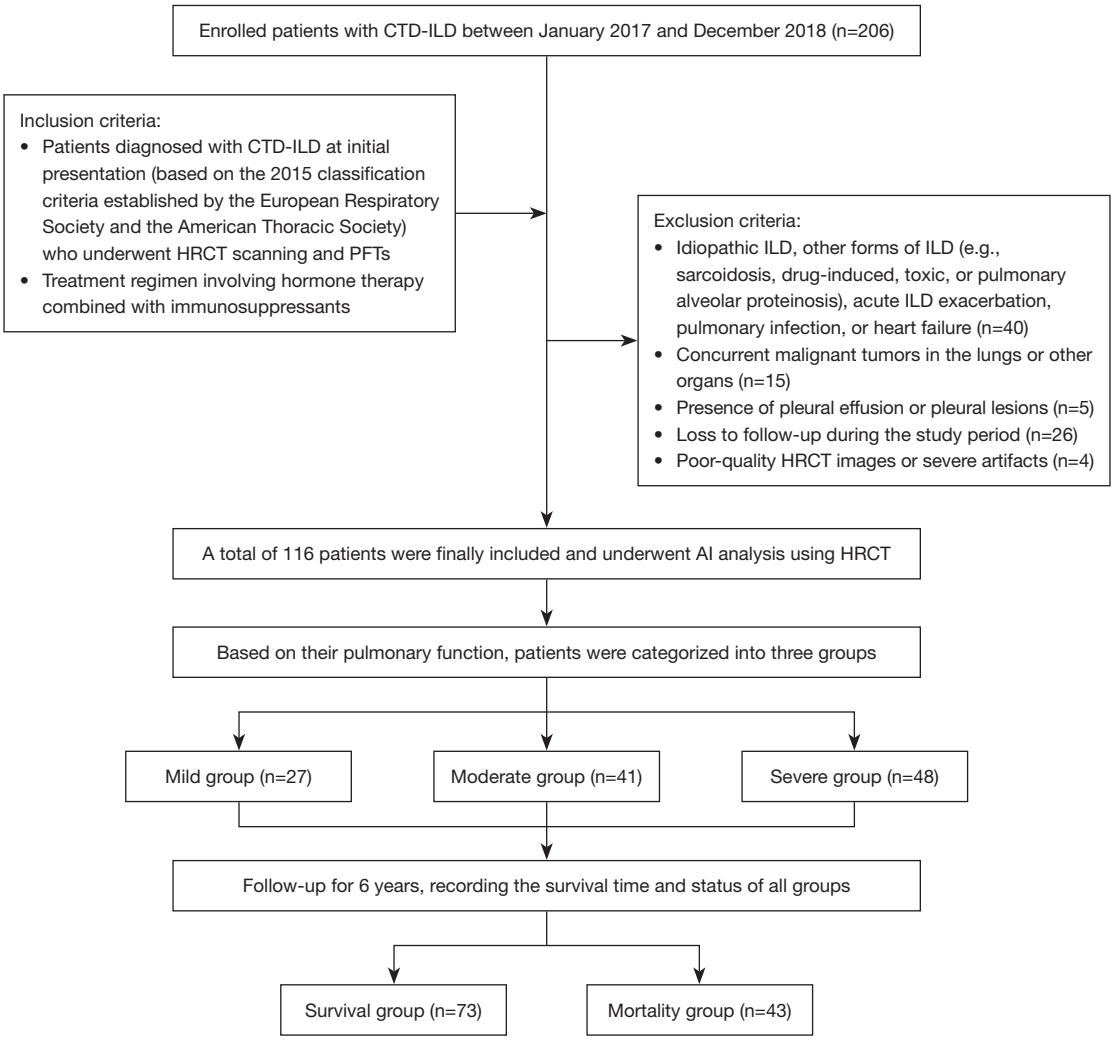

Figure 1 The flowchart of this research. AI, artificial intelligence; CTD-ILD, connective tissue disease-associated interstitial lung disease; HRCT, high-resolution computed tomography; ILD, interstitial lung disease; PFT, pulmonary function test.

patients diagnosed with CTD-ILD at initial presentation (based on the 2015 classification criteria established by the European Respiratory Society and the American Thoracic Society) who underwent HRCT scanning and PFT. (II) Treatment regimen involving systemic glucocorticoids combined with immunosuppressants. The systemic glucocorticoids encompassing prednisone and methylprednisolone. Meanwhile, the category of "immunosuppressants" includes cyclosporine A, tacrolimus, mycophenolate mofetil, hydroxychloroquine sulfate, tripterygium glycosides tablets, leflunomide, and total glucosides of peony. Exclusion criteria: (I) idiopathic ILD, other forms of ILD (e.g., sarcoidosis, drug-induced, toxic, or pulmonary alveolar proteinosis), acute ILD exacerbation, pulmonary infection, or heart failure. (II) Concurrent malignant tumors in the lungs or other organs. (III) Presence of pleural effusion or pleural lesions. (IV) Loss to follow-up during the study period. (V) Poor-quality HRCT images or severe artifacts.

The final cohort comprised 116 patients (24 male, 92 female), with a mean age of 58.6±11.4 years (range, 28.0–84.0 years).

The flowchart of this study is shown in *Figure 1*.

CT examination

All patients underwent imaging with a 128-slice CT scanner (GE Revolution, Boston, MA, USA). The scanning

parameters were as follows: tube voltage of 120 kV with automatic tube current modulation, detector width of 128 mm × 0.625 mm, pitch of 0.992, and gantry rotation time of 0.5 seconds per rotation. The scan coverage extended from the thoracic inlet to the lung base, extending caudally by 1 to 1.5 vertebral body lengths. Image reconstruction was performed using adaptive statistical iterative reconstruction, with a lung window slice thickness of 1.25 mm and a slice interval of 1.25 mm.

Pulmonary function

To comprehensively evaluate pulmonary function status, we constructed a composite pulmonary function grade that integrates two core lung function metrics: forced vital capacity percentage predicted (FVC%) and diffusing capacity for carbon monoxide percentage predicted (DLCO%). The specific grading criteria are outlined as follows:

- Mild group: FVC% ≥70% and DLCO% ≥70%.
- Moderate group: FVC% ≥50% and <70%, and/or DLCO% ≥40% and <70%.
- Severe group: FVC% <50% and/or DLCO% <40%. The interval between PFTs and CT scans did not exceed 3 days for any patient.

Patients follow-up

The observation period commenced at the time of the patient's initial HRCT examination and spanned 72 months of follow-up. The clinical endpoint was defined as patient overall mortality.

AI analysis

This study employed an AI analysis system developed by Shanghai United Imaging Medical Technology Co., Ltd. (Shanghai, China). The system enhances diagnostic sensitivity and accuracy through a multi-stage framework and multi-modal data fusion, enabling more effective assessment and prediction of disease progression (8). Based on deep learning algorithms, the system rapidly performs full-volume integration and segmentation of HRCT images, followed by quantitative analysis of the lungs (left and right) and pulmonary lesion areas (lesion and non-lesion regions). It provides the following parameters: Total lung volume, left lung volume, and right lung volume; lesion volume and its percentage relative to the total lung, left lung, and right lung; volume and percentage of lesion components within specific CT value ranges: ≤–751, –750 to –301, –300 to 49, and ≥50 Hounsfield units (HU). In total, 17 parameters are obtained. Representative AI-generated images are presented in *Figure 2*.

Statistical analyses

All statistical analyses were performed using SPSS 22.0 software (SPSS Inc.), with statistical significance set at $P<0.05$. Continuous variables were analyzed using independent *t*-tests or Mann-Whitney *U* tests, depending on their distributional normality, while categorical variables were assessed using chi-square tests or Fisher's exact tests. Differences in the 17 AI parameters across the three groups (mild, moderate, and severe) were evaluated using one-way analysis of variance (ANOVA) followed by least significant difference (LSD) post hoc pairwise comparisons. The Spearman rank correlation test was employed to examine the association between the 17 AI parameters and the composite pulmonary function grades. Overall survival rates among the mild, moderate, and severe groups were analyzed using Kaplan-Meier curves, with intergroup differences assessed via the log-rank test and multifactorial ANOVA. Univariate analysis and Cox proportional-hazards regression were used to assess the association between AI-derived parameters and prognosis. Univariate analyses were performed for all 17 AI-derived parameters included in the study. Candidate variables for the multivariable Cox proportional hazards regression model were selected based on two criteria: their established clinical relevance to the outcome and/or a statistically significant association ($P<0.05$) identified in the univariate analysis. A forced entry approach was subsequently employed to assess the independent association of each candidate variable with the primary study outcome. All results from these analyses are reported as hazard ratios (HRs) accompanied by 95% confidence intervals (CIs).

Results

The demographic and clinical information

A comprehensive baseline characteristics table that details demographics and key clinical variables for the entire cohort (*Table 1*).

The demographic information of the three different PFT groups is as follows:

(I) Mild group: n=27; 4 males, 23 females; mean age

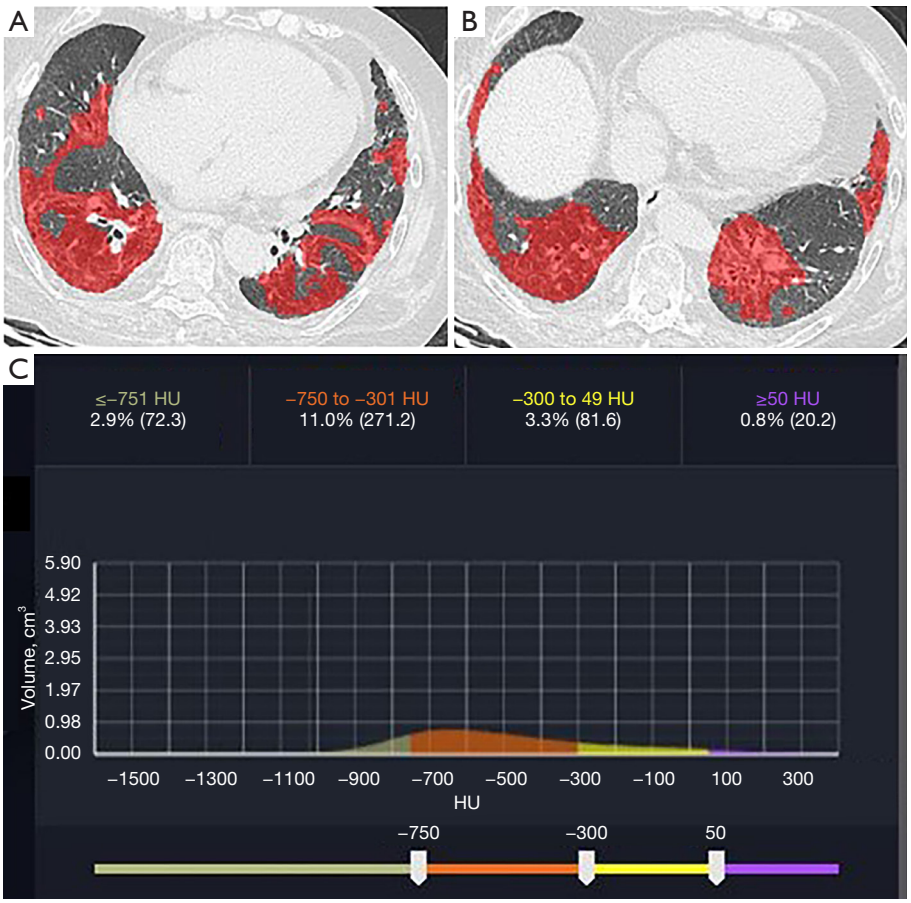

Figure 2 Representative AI images. A 75-year-old male patient with CTD-ILD. (A,B) Two HRCT slices, with the red regions indicating lung lesions automatically identified by AI. (C) A histogram of CT values from the lung lesions. AI, artificial intelligence; CT, computed tomography; CTD-ILD, connective tissue disease-associated interstitial lung disease; HRCT, high-resolution computed tomography; HU, Hounsfield units.

56.3±10.9 years (range, 28.0–76.0 years);

(II) Moderate group: n=41; 7 males, 34 females; mean age 57.8±13.3 years (range, 28.0–84.0 years);

(III) Severe group: n=48; 13 males, 35 females; mean age 60.6±9.7 years (range, 45.0–77.0 years).

The differences in AI parameters across the three groups

The 17 AI parameters exhibited significant variations across the three groups (all P<0.001), with group-specific differences detailed in *Table 2*.

The Spearman correlation analysis of AI parameters and pulmonary function grades

The 17 AI parameters were significantly correlated with pulmonary function, and the results are shown in *Table 3*.

The analysis of overall survival rates for patients

The Kaplan-Meier curve analysis revealed that the overall survival rates for the three groups were 96.3%, 73.2%, and 35.4%, respectively. The log-rank test demonstrated a statistically significant difference (P<0.001). The overall survival analysis function curves of the three groups are shown in *Figure 3*.

The univariate and Cox proportional-hazards regression

The results of the univariate regression analysis for distinguishing the survival group and mortality group are presented in *Table 4*. The Cox proportional-hazards

Table 1 Baseline characteristics of the study population stratified by survival status

Characteristics	Overall cohort (n=116)	Survival group (n=73)	Mortality group (n=43)	P value
Demographics				
Age (years)	58.6±11.4 (28.0–84.0)	55.7±11.3 (28.0–84.0)	63.6±9.8 (45.0–78.0)	<0.001*
Female	92 (79.3)	55 (75.3)	37 (86.0)	0.24
CTD subtype				0.38
pSS	59 (50.9)	39 (53.4)	20 (46.5)	
RA	18 (15.5)	8 (11.0)	10 (23.3)	
SLE	13 (11.2)	9 (12.3)	4 (9.3)	
Other CTDs[†]	26 (22.4)	17 (23.3)	9 (20.9)	
Composite pulmonary function[‡]				0.001*
Mild group	27 (23.3)	26 (35.6)	1 (2.3)	
Moderate group	41 (35.3)	30 (41.2)	11 (25.6)	
Severe group	48 (41.4)	17 (23.3)	31 (72.1)	
HRCT pattern[§]				<0.001*
NSIP	74 (63.8)	54 (74.0)	20 (46.5)	
UIP	18 (15.5)	4 (5.5)	14 (32.6)	
Mixed pattern of UIP and NSIP	9 (7.8)	3 (4.1)	6 (14.0)	
Interminate	10 (8.6)	8 (11.0)	2 (4.7)	
Other patterns	5 (4.3)	4 (5.5)	1 (2.3)	
Smoking status				0.77
Never-smoker	103 (88.8)	64 (87.7)	39 (90.7)	
Former-smoker	13 (11.2)	9 (12.3)	4 (9.3)	
Disease history				
Duration (years)	2.5±2.7 (0.1–15.0)	2.4±2.9 (0.1–15.0)	2.8±2.3 (0.1–8.0)	0.40
Treat at baseline				0.28
Glucocorticoids	18 (15.5)	13 (17.8)	5 (11.6)	
Immunosuppressants[¶]	7 (6.0)	6 (14.0)	1 (2.3)	
Glucocorticoids combined with immunosuppressants	91 (78.4)	54 (74.0)	37 (86.0)	

Continuous data are presented as mean ± SD (range); categorical data are presented as percentage. [†], other CTDs comprise dermatomyositis, anti-synthetase syndrome, anti-Jo-1 syndrome, polymyositis, ANCA-associated vasculitis, systemic sclerosis, undifferentiated CTD, and mixed CTD. [‡], the composite pulmonary-function grade integrates FVC% and DLCO% as follows: mild group: FVC% ≥70% and DLCO% ≥70%; moderate group: FVC% ≥50% and <70%, and/or DLCO% ≥40% and <70%; severe group: FVC% <50% and/or DLCO% <40%. [§], additional HRCT patterns include combined NSIP + LIP, NSIP + OP, and isolated LIP. [¶], immunosuppressants encompass cyclosporine A, tacrolimus, mycophenolate mofetil, hydroxychloroquine sulfate, Tripterygium glycosides tablets, leflunomide, and total glucosides of peony. *, P<0.05. ANCA, anti-neutrophil cytoplasmic antibody; CTD, connective tissue disease; DLCO%, diffusing capacity for carbon monoxide percentage predicted; FVC%, forced vital capacity percentage predicted; HRCT, high-resolution computed tomography; LIP, lymphocytic interstitial pneumonia; NSIP, non-specific interstitial pneumonia; OP, organizing pneumonia; pSS, primary Sjögren's syndrome; RA, rheumatoid arthritis; SD, standard deviation; SLE, systemic lupus erythematosus; UIP, usual interstitial pneumonia.

Table 2 Differences of AI parameters among the three groups with mild, moderate, and severe composite pulmonary function grades

AI parameters	Mild (n=27) *vs.* moderate (n=41)		Mild (n=27) *vs.* severe (n=48)		Moderate (n=41) *vs.* severe (n=48)	
	Difference	P value	Difference	P value	Difference	P value
Volume of total lung (cm^3)	3,230.2 *vs.* 2,700.9	0.008*	3,230.2 *vs.* 2,430.2	<0.001***	2,700.9 *vs.* 2,430.2	0.11
Volume of left lung (cm^3)	1,454.1 *vs.* 1,195.9	0.007*	1,454.1 *vs.* 1,060.6	<0.001***	1,195.9 *vs.* 1,060.6	0.10
Volume of right lung (cm^3)	1,776.1 *vs.* 1,505.1	0.01*	1,776.1 *vs.* 1,369.6	<0.001***	1,505.1 *vs.* 1,369.6	0.14
Volume of total lung infection (cm^3)	249.9 *vs.* 313.6	0.37	249.9 *vs.* 618.8	<0.001***	313.6 *vs.* 618.8	<0.001***
Percentage of total lung infection (%)	8.6 *vs.* 12.3	0.10	8.6 *vs.* 25.2	<0.001***	12.3 *vs.* 25.2	<0.001***
Volume of left lung infection (cm^3)	103.2 *vs.* 138.7	0.31	103.2 *vs.* 281.8	<0.001***	138.7 *vs.* 281.8	<0.001***
Percentage of left lung infection (%)	8.3 *vs.* 12.4	0.10	8.3 *vs.* 26.1	<0.001***	12.4 *vs.* 26.1	<0.001***
Volume of right lung infection (cm^3)	146.7 *vs.* 174.9	0.47	146.7 *vs.* 337.0	<0.001***	174.9 *vs.* 337.0	<0.001***
Percentage of right lung infection (%)	9.0 *vs.* 12.4	0.17	9.0 *vs.* 24.8	<0.001***	12.4 *vs.* 24.8	<0.001***
Volume of infection component (cm^3)						
≤−751 HU	77.5 *vs.* 65.9	0.68	77.5 *vs.* 138.2	0.03*	65.9 *vs.* 138.2	0.003***
−750 to −301 HU	130.0 *vs.* 158.2	0.47	130.0 *vs.* 308.3	<0.001***	158.2 *vs.* 308.3	<0.001***
−300 to 49 HU	34.1 *vs.* 68.8	0.006*	34.1 *vs.* 130.7	<0.001***	68.8 *vs.* 130.7	<0.001***
≥50 HU	8.4 *vs.* 20.7	0.007*	8.4 *vs.* 41.6	<0.001***	20.7 *vs.* 41.6	<0.001***
Percentage of infected components (%)						
≤−751 HU	2.3 *vs.* 2.4	0.94	2.3 *vs.* 5.0	0.001**	2.4 *vs.* 5.0	<0.001***
−750 to −301 HU	4.6 *vs.* 6.2	0.23	4.6 *vs.* 12.5	<0.001***	6.2 *vs.* 12.5	<0.001***
−300 to 49 HU	1.3 *vs.* 2.9	0.02*	1.3 *vs.* 5.8	<0.001***	2.9 *vs.* 5.8	<0.001***
≥50 HU	1.3 *vs.* 2.9	0.02*	0.29 *vs.* 1.9	<0.001***	0.86 *vs.* 1.9	<0.001***

Data are presented as difference (P value). *, P<0.05; **, P<0.005; ***, P<0.001. AI, artificial intelligence; HU, Hounsfield units.

regression revealed that the two most important factors were left lung volume and the percentage of disease components ≤−751 HU, which were protective factors and risk factors for overall survival rate, respectively. The specific parameters can be found in *Table 5*.

Discussion

This study employed an AI-based lung lesion analysis system to investigate a novel quantitative approach for predicting the prognosis of CTD-ILD using HRCT. The findings demonstrated that the survival rate in the mild lung function group was significantly higher than in both the moderate and severe groups, while the moderate group also exhibited a significantly higher survival rate than the severe group. The Cox proportional-hazards regression obtained two key parameters: the volume of the left lung and the percentage of affected components ≤−751 HU (%).

The imaging patterns and extent of involvement often reflect disease progression and poor prognosis. Computer-based quantitative indicators can effectively assess the degree of lung damage in patients with CTD-ILD (10). In our study, we employed a deep learning algorithm to classify and evaluate pathological lung components, yielding a total of 17 quantitative parameters. Univariate analysis of AI-derived parameters revealed that patients in the mortality group exhibited significantly higher parenchymal involvement volumes and percentages across the entire lung, left lung, and right lung compared to the survival group. Conversely, the total lung, left lung, and right lung volumes in the mortality group were markedly smaller than those in the survival group. This observation may be attributed to advanced pulmonary fibrosis in late-stage interstitial pneumonia, which leads to progressive

Table 3 Spearman correlation analysis of 17 AI parameters and composite pulmonary function grades

AI parameters	Correlation coefficient	P value
Volume of total lung (cm^3)	−0.374†	<0.001
Volume of left lung (cm^3)	−0.372†	<0.001
Volume of right lung (cm^3)	−0.350†	<0.001
Volume of total lung infection (cm^3)	0.500‡	<0.001
Percentage of total lung infection (%)	0.646‡	<0.001
Volume of left lung infection (cm^3)	0.514‡	<0.001
Percentage of left lung infection (%)	0.649‡	<0.001
Volume of right lung infection (cm^3)	0.490‡	<0.001
Percentage of right lung infection (%)	0.591‡	<0.001
Volume of infection component (cm^3)		
≤−751 HU	0.276†	0.003
−750 to −301 HU	0.447‡	<0.001
−300 to 49 HU	0.654‡	<0.001
≥50 HU	0.683‡	<0.001
Percentage of infected components (%)		
≤−751 HU	0.415‡	<0.001
−750 to −301 HU	0.584‡	<0.001
−300 to 49 HU	0.665‡	<0.001
≥50 HU	0.695‡	<0.001

†, low degree of linear correlation; ‡, significant correlation. AI, artificial intelligence; HU, Hounsfield units.

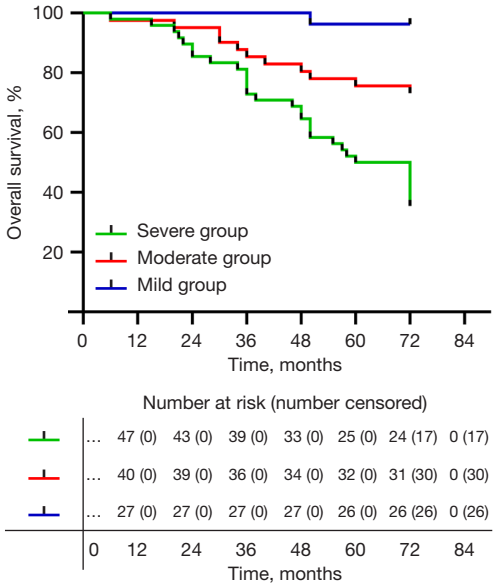

Figure 3 Overall survival function curves of the mild, moderate, and severe groups. The blue line represents the mild group, the red line represents the moderate group, and green line represents the severe group.

lung volume reduction (11). Supporting our findings, Si-Mohamed *et al.* demonstrated that deep learning-based lung volume measurements in longitudinal CT scans correlate with lung function, where greater volume loss is associated with poorer prognosis (12). Notably, left lung volume served as a protective factor for survival in CTD-ILD patients—larger volumes correlated with better prognosis, while smaller volumes indicated worse outcomes. We speculate that the left lung, being anatomically smaller than the right, is more susceptible to damage and exhibits more pronounced volume reduction in the presence of pathology. Consequently, left lung volume may serve as a more reliable prognostic marker than right lung volume. This aligns with the findings of Yin *et al.* (13), who reported that in quantitative CT assessments of ILD patients, volumetric measurements of the entire lung, left lung, and individual lobes (excluding the right middle lobe) hold greater predictive value.

The mortality group exhibited significantly higher values than the survival group in the following parameters: the percentage of lesion volume ≤−751 HU, the percentage of lesion components ranging from −750 to −301 HU, and the volumes and percentages of lesion components within −300 to 49 HU as well as those ≥50 HU. In previous studies, Carvalho *et al.* (14) defined pulmonary lesions with CT values between −500 and 50 HU as ground-glass opacities. HRCT findings in interstitial pneumonia typically include ground-glass opacities, reticular patterns, linear shadows, and honeycombing. Ground-glass opacities are more prevalent in the early acute inflammatory phase, primarily due to alveolar edema and inflammatory cell infiltration, indicating an intensified pulmonary inflammatory response (15). Generally, ground-glass opacities observed on HRCT reflect inflammatory processes within the pulmonary interstitium or alveolar spaces, particularly in the non-specific interstitial pneumonia (NSIP) subtype. Histopathologically, these opacities may represent early-stage pulmonary interstitial fibrosis. Studies have demonstrated that while ground-glass opacities in rheumatoid arthritis (RA) ILD patients may resolve on follow-up CT scans, they more frequently progress to

Table 4 Univariate analysis of prognosis in CTD-ILD patients

AI parameters	Survival group (n=73)	Mortality group (n=43)	P value
Volume of total lung (cm^3)	3,097.0 (2,482.9–3,622.7)	2,050.5 (1,653.1–2,357.7)	<0.001***
Volume of left lung (cm^3)	1,417.8 (1,061.5–16,615)	858.3 (699.6–1,054)	<0.001***
Volume of right lung (cm^3)	16,930 (1,347.1–1,974.3)	1,171.6 (926.1–1,371.8)	<0.001***
Volume of total lung infection (cm^3)	341.5 (171.8–516.2)	406.7 (304.6–598.4)	0.13
Percentage of total lung infection (%)	11.6 (3.9–18.9)	19.6 (15.4–27.7)	<0.001***
Volume of left lung infection (cm^3)	156.5 (56.4–225.4)	181.0 (134.5–234.2)	0.23
Percentage of left lung infection (%)	11.6 (4.3–18.5)	22.0 (15.5–32.0)	<0.001***
Volume of right lung infection (cm^3)	177.9 (80.0–293.8)	248.5 (157.8–345.8)	0.09
Percentage of right lung infection (%)	12.2 (3.9–19.5)	19.6 (15.3–27.2)	<0.001***
Volume of infection component (cm^3)			
≤–751 HU	61.0 (29.5–136.6)	60.0 (31.3–113.9)	0.77
–750 to –301 HU	155.3 (68.1–291.0)	195.2 (153.3–285.6)	0.29
–300 to 49 HU	57.5 (18.7–100.3)	100.4 (68.9–152.3)	0.002**
≥50 HU	15.8 (6.25–32)	28.3 (19.0–45.8)	0.001***
Percentage of infected components (%)			
≤–751 HU	2.0 (1.2–4.1)	3.2 (1.7–5.1)	0.02*
–750 to –301 HU	6.0 (1.7–9.6)	11.0 (7.9–13.1)	<0.001***
–300 to 49 HU	2.0 (0.6–4.2)	5.6 (3.0–7.4)	<0.001***
≥50 HU	0.5 (0.2–1.0)	1.6 (0.8–2.2)	<0.001***

Data are presented as median (interquartile range) for continuous variables. *, P<0.05; **, P<0.005; ***, P<0.001. AI, artificial intelligence; CTD-ILD, connective tissue disease-associated interstitial lung disease; HU, Hounsfield units.

Table 5 Cox proportional-hazards regression parameters

Factors	β	Standard error	Wald	HR (95% CI)	P value
Volume of left lung	–0.004	0.001	43.151	0.996 (0.994–0.997)	<0.001
Percentage of infected components ≤–751 HU (%)	0.246	0.043	32.766	1.280 (1.176–1.392)	<0.001

β, regression coefficient; CI, confidence interval; HR, hazard ratio; HU, Hounsfield units.

fibrotic changes with honeycombing (16). However, no statistically significant difference was observed between the mortality and survival groups regarding the volume of pathological components ≤–751 HU. We hypothesize that components ≤–751 HU comprise a heterogeneous mixture, potentially including ground-glass opacities and other mixed-density shadows. Therefore, we propose that percentage-based assessment may serve as a more reliable predictive factor.

Traditional HRCT, widely employed in clinical practice to diagnose subtle structural lung changes and evaluate lesion extent and severity, relies heavily on radiologists' subjective observations, introducing significant variability. In contrast, quantitative HRCT indicators serve as more objective and convenient prognostic tools, demonstrating greater stability despite disease progression. These metrics hold substantial clinical significance for diagnosis and treatment. This study pioneers the use of an AI-analysis system to perform quantitative HRCT image analysis, further dissecting lesion components.

There are several limitations in this study. First, small sample size and single-center design. Second, the scanning technicians in this study were not fixed, but all adopted standard scanning and reconstruction algorithms. Third, the follow-up period was relatively short. Fourth, retrospective nature of the study. Fifth, absence of external validation for AI-derived parameters. Future research should address these limitations by employing a larger sample size and extended observation periods.

Conclusions

This study demonstrates the prognostic value of AI-based quantitative HRCT analysis in CTD-ILD. Two key imaging biomarkers were identified as independent predictors of overall survival: left lung volume (protective factor) and the percentage of disease components with attenuation ≤–751 HU (risk factor). These findings support the integration of objective, automated quantitative imaging parameters for improved risk stratification in CTD-ILD patients, complementing conventional assessment methods. Further validation in larger cohorts is warranted to develop predictive models incorporating these biomarkers for clinical application.

Acknowledgments

The authors acknowledge the technicians and nursing teams of the Department of Radiology, Nanjing Drum Tower Hospital, Affiliated Hospital of Medical School, Nanjing University for their assistance in data collection.

Footnote

Reporting Checklist: The authors have completed the STROBE reporting checklist. Available at https://jtd.amegroups.com/article/view/10.21037/jtd-2025-1827/rc

Data Sharing Statement: Available at https://jtd.amegroups.com/article/view/10.21037/jtd-2025-1827/dss

Peer Review File: Available at https://jtd.amegroups.com/article/view/10.21037/jtd-2025-1827/prf

Funding: This work was supported by the fundings for Clinical Trials from the Affiliated Drum Tower Hospital, Medical School of Nanjing University (No. 2023-LCYJ-PY-26 to X.X.), the Nanjing Health Science and Technology Development Special Fund Major Project (No. ZKX22015 to X.X.), the Key Projects for the Development of New Medical Technologies from the Affiliated Drum Tower Hospital, Medical School of Nanjing University (No. XJSFZLX202313 to X.X.), and the Double Innovation PhD Project in "Jiangsu Province High-Level Innovation and Entrepreneurship Talent Introduction Plan" (No. JSSCBS20211495 to C.C.).

Conflicts of Interest: All authors have completed the ICMJE uniform disclosure form (available at https://jtd.amegroups.com/article/view/10.21037/jtd-2025-1827/coif). C.C. reports support from the Double Innovation PhD Project in "Jiangsu Province High-level Innovation and Entrepreneurship Talent Introduction Plan" (No. JSSCBS20211495). X.X. reports support from Clinical Trials from the Affiliated Drum Tower Hospital, Medical School of Nanjing University (No. 2023-LCYJ-PY-26), the Nanjing Health Science and Technology Development Special Fund Major Project (No. ZKX22015), and the Key Projects for the Development of New Medical Technologies from the Affiliated Drum Tower Hospital, Medical School of Nanjing University (No. XJSFZLX202313). Y.W. and F.S. are employees of Shanghai United Imaging Intelligence Co., Ltd. The company has no role in designing and performing the surveillances and analyzing and interpreting the data. The other authors have no conflicts of interest to declare.

Ethical Statement: The authors are accountable for all aspects of the work in ensuring that questions related to the accuracy or integrity of any part of the work are appropriately investigated and resolved. This study was conducted in accordance with the Declaration of Helsinki and its subsequent amendments. The study was approved by the Ethics Committee of Nanjing Drum Tower Hospital (No. 2022-449-02) and informed consent was obtained from the participants' next of kin or directly from the patients.

References

1. Storrer KM, Müller CS, Pessoa MCA, et al. Connective tissue disease-associated interstitial lung disease. J Bras Pneumol 2024;50:e20230132.
2. Joy GM, Arbiv OA, Wong CK, et al. Prevalence, imaging patterns and risk factors of interstitial lung disease in connective tissue disease: a systematic review and meta-analysis. Eur Respir Rev 2023;32:220210.
3. Maher TM. Interstitial Lung Disease: A Review. JAMA 2024;331:1655-65.
4. Fan JJ, Gu JM, Xiao SY, et al. Risk factors for progression of pulmonary fibrosis: a single-centered, retrospective study. Front Med (Lausanne) 2024;11:1335758.
5. Chiu YH, Spierings J, de Jong PA, et al. Predictors for progressive fibrosis in patients with connective tissue disease associated interstitial lung diseases. Respir Med 2021;187:106579.
6. Chen J, Yang Z, Yuan Q, et al. Prediction models for pulmonary function during acute exacerbation of chronic obstructive pulmonary disease. Physiol Meas 2021;41:125010.
7. Chen L, Zhu M, Lu H, et al. Quantitative evaluation of disease severity in connective tissue disease-associated interstitial lung disease by dual-energy computed tomography. Respir Res 2022;23:47.
8. Wang C, Shao J, He Y, et al. Data-driven risk stratification and precision management of pulmonary nodules detected on chest computed tomography. Nat Med 2024;30:3184-95.
9. Shan F, Gao Y, Wang J, et al. Abnormal lung quantification in chest CT images of COVID-19 patients with deep learning and its application to severity prediction. Med Phys 2021;48:1633-45.
10. Chen A, Karwoski RA, Gierada DS, et al. Quantitative CT Analysis of Diffuse Lung Disease. Radiographics 2020;40:28-43.
11. Sun H, Liu M, Kang H, et al. Quantitative analysis of high-resolution computed tomography features of idiopathic pulmonary fibrosis: a structure-function correlation study. Quant Imaging Med Surg 2022;12:3655-65.
12. Si-Mohamed SA, Nasser M, Colevray M, et al. Automatic quantitative computed tomography measurement of longitudinal lung volume loss in interstitial lung diseases. Eur Radiol 2022;32:4292-303.
13. Yin N, Shen C, Dong F, et al. Computer-aided identification of interstitial lung disease based on computed tomography. J Xray Sci Technol 2019;27:591-603.
14. Carvalho ARS, Guimarães AR, Sztajnbok FR, et al. Automatic Quantification of Interstitial Lung Disease From Chest Computed Tomography in Systemic Sclerosis. Front Med (Lausanne) 2020;7:577739.
15. Kadura S, Raghu G. Rheumatoid arthritis-interstitial lung disease: manifestations and current concepts in pathogenesis and management. Eur Respir Rev 2021;30:210011.
16. Yamakawa H, Sato S, Nishizawa T, et al. Impact of radiological honeycombing in rheumatoid arthritis-associated interstitial lung disease. BMC Pulm Med 2020;20:25.

Cite this article as: Chu C, Yan A, Xu J, Hu J, Wei Y, Shi F, Zhao S, Xin X. Association of artificial intelligence-based high-resolution computed tomography parameters with all-cause mortality in patients with connective tissue disease-associated interstitial lung disease: a longitudinal cohort study. J Thorac Dis 2026;18(1):14. doi: 10.21037/jtd-2025-1827